Epitaxial Growth Development

Cooperative Research and Development Final Report

CRADA Number: CRD-18-00755

NREL Technical Contact: Kirstin Alberi

NREL is a national laboratory of the U.S. Department of Energy
Office of Energy Efficiency & Renewable Energy
Operated under Contract No. DE-AC36-08GO28308

This report is available at no cost from
NREL at www.nrel.gov/publications.

Technical Report
NREL/TP-5K00-94079
July 2025

Epitaxial Growth Development

Cooperative Research and Development Final Report

CRADA Number: CRD-18-00755

NREL Technical Contact: Kirstin Alberi

Suggested Citation
Alberi, Kirstin. 2025. *Epitaxial Growth Development: Cooperative Research and Development Final Report, CRADA Number CRD-18-00755.* Golden, CO: National Renewable Energy Laboratory. NREL/TP-5K00-94079.
https://www.nrel.gov/docs/fy25osti/94079.pdf.

NREL is a national laboratory of the U.S. Department of Energy
Office of Energy Efficiency & Renewable Energy
Operated under Contract No. DE-AC36-08GO28308

This report is available at no cost from
NREL at www.nrel.gov/publications.

Technical Report
NREL/TP-5K00-94079
July 2025

15013 Denver West Parkway
Golden, CO 80401
303-275-3000 • www.nrel.gov

NOTICE

This work was authored by NREL for the U.S. Department of Energy (DOE), operated under Contract No. DE-AC36-08GO28308. Funding provided by the U.S. Department of Energy Office of Energy Efficiency and Renewable Energy Advanced Manufacturing and Materials Technologies Office. The views expressed herein do not necessarily represent the views of the DOE or the U.S. Government.

This work was prepared as an account of work sponsored by an agency of the United States Government. Neither the United States Government nor any agency thereof, nor any of their employees, nor any of their contractors, subcontractors or their employees, makes any warranty, express or implied, or assumes any legal liability or responsibility for the accuracy, completeness, or any third party's use or the results of such use of any information, apparatus, product, or process disclosed, or represents that its use would not infringe privately owned rights. Reference herein to any specific commercial product, process, or service by trade name, trademark, manufacturer, or otherwise, does not necessarily constitute or imply its endorsement, recommendation, or favoring by the United States Government or any agency thereof or its contractors or subcontractors. The views and opinions of authors expressed herein do not necessarily state or reflect those of the United States Government or any agency thereof, its contractors or subcontractors.

This report is available at no cost from NREL at www.nrel.gov/publications.

U.S. Department of Energy (DOE) reports produced after 1991 and a growing number of pre-1991 documents are available free via www.OSTI.gov.

Cover photos (clockwise from left): Josh Bauer, NREL 61725; Visualization from the NREL Insight Center; Getty-181828180; Agata Bogucka, NREL 91683; Dennis Schroeder, NREL 51331; Werner Slocum, NREL 67842.

NREL prints on paper that contains recycled content.

Cooperative Research and Development Final Report

Report Date: March 13, 2025

In accordance with requirements set forth in the terms of the CRADA agreement, this document is the CRADA final report, including a list of subject inventions, to be forwarded to the DOE Office of Scientific and Technical Information as part of the commitment to the public to demonstrate results of federally funded research.

Parties to the Agreement: Trumpf Photonics, Inc

CRADA Number: CRD-18-00755

CRADA Title: Epitaxial Growth Development

Responsible Technical Contact at NREL:

Kirstin Alberi | Kirstin.Alberi@nrel.gov

Name and Email Address of POC at Company:

Valentin Loyo-Maldonado | valentin.loyo-maldonado@trumpf.com

Sponsoring DOE Program Office(s):

Office of Energy Efficiency and Renewable Energy (EERE), Advanced Manufacturing and Materials Technologies Office

Joint Work Statement Funding Table showing DOE commitment:

Estimated Costs	NREL Shared Resources a/k/a Government In-Kind
Year 1	$350,000.00
Year 2, Modification #1	$350,000.00
Year 3, Modification #2	$350,000.00
Year 4, Modification #3	$.00
TOTALS	$1,050,000.00

Executive Summary of CRADA Work:

The purpose of this CRADA is to assist Trumpf Photonics in developing a procedure to grow ZnSe epilayers on the (110) facets of AlGaAs/InGaAs laser diodes that will provide high degrees of electronic passivation and performance reliability. Work will be divided into four tasks: 1) characterization of material growth at Trumpf Photonics, 2) development of a highly effective AlGaAs facet cleaning procedure at NREL, 3) development of a ZnSe epitaxy procedure at NREL, and 4) transfer of the procedures developed at NREL to the Trumpf Photonics site. This CRADA is designed to last 3 years total.

This report is available at no cost from NREL at www.nrel.gov/publications.

CRADA benefit to DOE, Participant, and US Taxpayer:

- Assists laboratory in achieving programmatic scope
- enhances the laboratory's core competencies,
- enhances U.S. competitiveness by utilizing DOE developed intellectual property and/or capabilities.

Summary of Research Results:

Statement of work from CRADA document

NREL will work with Trumpf Photonics to develop a procedure for epitaxially growing a ZnSe passivation layer on cleaved AlGaAs/InGaAs (110) facets. This work involves four major tasks: 1) characterization of material growth at Trumpf Photonics, 2) development of a highly effective AlGaAs facet cleaning procedure, 3) development of a ZnSe epitaxy procedure, and 4) transfer of the procedures to Trumpf. Details of the work included in each task are listed in the following section.

Task 1: Characterization of Trumpf material

Trumpf Photonics currently grows ZnSe epilayers on cleaved (110) facets of their AlGaAs/InGaAs laser structures by molecular beam epitaxy (MBE). NREL will characterize these structures via a variety of structural and optical characterization methods to understand how their growth procedure affects the properties of the AlGaAs/ZnSe interface. The primary questions to answer are 1) how well the cleaning procedure removes oxides from the AlGaAs surface before ZnSe epilayer growth; and 2) how the ZnSe epilayer initiation and bulk growth procedures affect the properties of the ZnSe and AlGaAs epilayers. This activity will include the following activities:

a. Structural characterization via x-ray diffraction (XRD), secondary ion mass spectrometry (SIMS) and x-ray photoemission spectroscopy (XPS) to determine the degree of oxygen contamination at the AlGaAs/ZnSe interface and the predominant bonding environment (i.e. Zn-As or (Al,Ga)-Se bonding)
b. Optical characterization via variable temperature photoluminescence (PL) and time-resolved photoluminescence (PL) to determine the optical quality of the ZnSe epilayer and passivation of the underlying AlGaAs layer. Cathodoluminescence (CL) will also be used to determine the spatial extent of oxide removal and density of extended defects.
c. Most of this characterization will be carried out on ZnSe grown on AlGaAs (110) wafers to assess the cleaning procedures. Some characterization will also be carried out on ZnSe grown on GaAs (110) wafers to remove the effects of Al on oxide removal and more carefully look at the ZnSe initiation conditions on the underlying GaAs properties.
d. The results obtained at NREL will also be correlated with transmission electron microscopy (TEM) analysis performed at Trumpf to understand the spatial extent of remaining oxide coverage at the ZnSe/AlGaAs interface.
e. Optical characterization (PL and CL) will be carried out on the ZnSe-coated (110) facets of full laser bars in order to correlate optical signatures of the interface with lifetime and other characterization measurements performed at Trumpf.

This report is available at no cost from NREL at www.nrel.gov/publications.

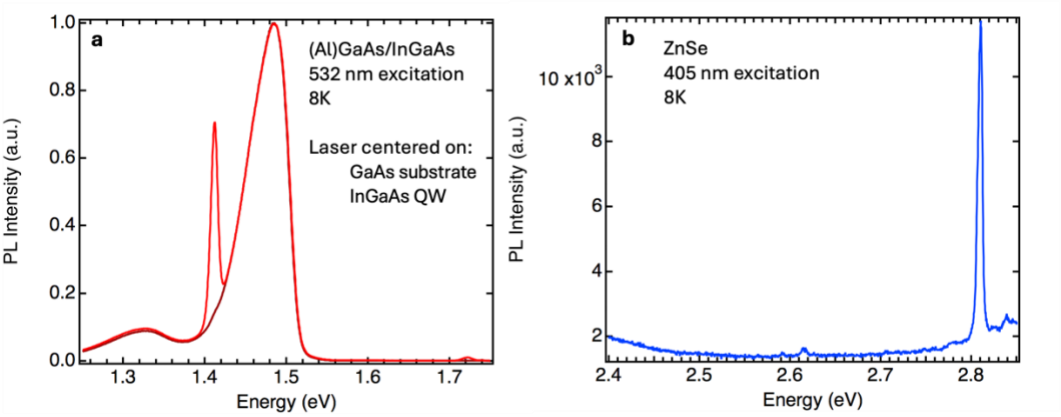

Figure 1. Representative photoluminescence (PL) measurements of laser bar facets at 8 K. The ZnSe and (Al)GaAs/InGaAs layers are probed with different lasers. a. PL spectra of the (Al)GaAs/InGaAs quantum well (QW) layers. The laser is focused on two different locations near and away from the InGaAs QW. b. PL spectrum of the ZnSe layer.

Oxygen contamination within the layers and interfaces of laser devices is well known to be correlated with early laser bar degradation and failure. Because the laser devices are exposed to air during various steps in their processing, there are opportunities for oxygen contamination to occur if the surfaces are not properly cleaned and prepared in vacuum prior to the next processing step. Work in this task primarily focused on understanding where that contamination occurs, how well it can be removed with proper surface preparation procedures, and the impact it has on laser bar performance. At the outset of this project, it was hypothesized that the most important surface to clean was the III-V (Al)GaAs/InGaAs

quantum well (QW) facet surface prior to ZnSe deposition, as oxygen defects located within the light-generating region of the device can act as non-radiative recombination sites and absorb laser light, which then leads to an increase in the device temperature and eventually causes catastrophic meltdown of the interface. Therefore, it is important to correlate the presence of oxygen contamination with device performance and lifetime. Evaluating other aspects, such as elemental intermixing across interfaces, is also another potential indicator of the formation of defects that may cause degradation by similar mechanisms.

Initial investigation of the ZnSe layers and ZnSe/III-V interfaces were carried out on a range of samples processed with varying ZnSe growth and hydrogen cleaning conditions and on differing structures, including GaAs and AlGaAs planar (110) substrates and in fully processed laser bars. PL was initially explored as a non-destructive characterization technique to obtain information about the ZnSe/(Al)GaAs interface and intermixing across the layers. More than 50 samples were measured as part of these studies. Representative PL spectra from the ZnSe layer and underlying (Al)GaAs/InGaAs quantum wells in full laser bars from one set of experiments are shown in Fig. 1. Subtle differences in the PL from the (Al)GaAs/InGaAs quantum wells were observed as a function of processing conditions but the differences were not large enough to reliably correlate to specific changes in the interface structure, oxygen contamination or elemental diffusion from the ZnSe into the III-V layers. ZnSe PL was only observed in a subset of samples in which the ZnSe layers were thick enough to emit measurable PL. Thus, PL was eventually discontinued as a tool for studying the ZnSe/(Al)GaAs interface. Similarly, CL did not produce enough emission from the ZnSe layers to examine extended defects and was also used in a limited capacity in other parts of this project.

This report is available at no cost from NREL at www.nrel.gov/publications.

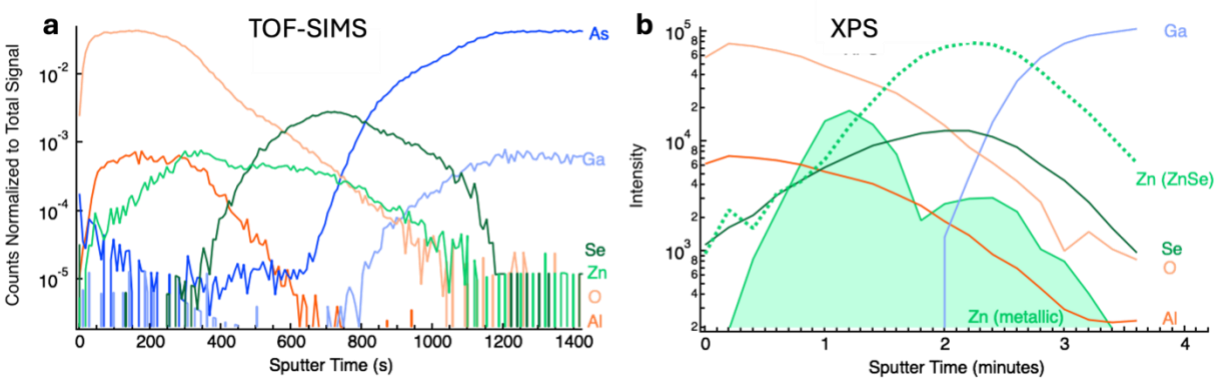

Figure 2. Representative elemental profiles in a Al2O3/ZnSe/GaAs stack grown on a planar GaAs substrate measured by a. Time of flight secondary ion mass spectrometry (TOF-SIMS), and b. x-ray photoemission spectroscopy (XPS).

XPS and time of flight (TOF) SIMS both provide depth-dependent information about composition at concentrations above and below the atomic percent level, respectively. Thus, information about oxygen impurities at the ZnSe/(Al)GaAs interface and elemental diffusion across it can be obtained. Because these measurements are difficult to perform on the small areas of the laser bar facets, they were initially carried out on large area planar wafers that went through the same processing conditions as typical laser bar facets. Figure 2 displays representative TOF SIMS and XPS measurements from a single sample. The data show that the elemental profiles are somewhat broad over the Al_2O_3/ZnSe/GaAs stack and roughly correlate with one another. XPS also provides information about the chemical state of each of the elements. The data in Fig. 2b indicates that Zn is found in two forms, corresponding to those in a ZnSe compound and metallic Zn. These two characterization techniques were used in many studies to understand the relationship between processing and chemistry at the Al_2O_3/ZnSe interface, which was later hypothesized to play an important role in laser bar performance (see below).

Laser bar samples were also examined with TEM at NREL to obtain more spatial information about the structure of the interfaces and the presence of oxygen contamination at interfaces. Figure 3 shows TEM micrographs and corresponding elemental profiles obtained with energy dispersive spectroscopy (EDS) from an as-grown laser bar. The images and profiles were measured in two different regions: 1) in an area near the InGaAs QW, which is surrounded by an AlGaAs waveguide with lower Al concentration, and 2) in an area slightly further away from the QW, which consists of an AlGaAs cladding layer with higher Al concentration. Both the TEM image and EDS profiles suggest that oxygen contamination in the region without Al, while significant oxygen contamination exists in the region with higher Al concentration. Oxygen bonds strongly with Al, and as a result, it is more difficult for the *in-situ* cleaning procedure to remove oxygen contamination from the surfaces of the cladding layers with high Al concentrations. The TEM and EDS measurements confirm that oxygen is still present in these regions, despite changes in III-V surface cleaning conditions.

This report is available at no cost from NREL at www.nrel.gov/publications.

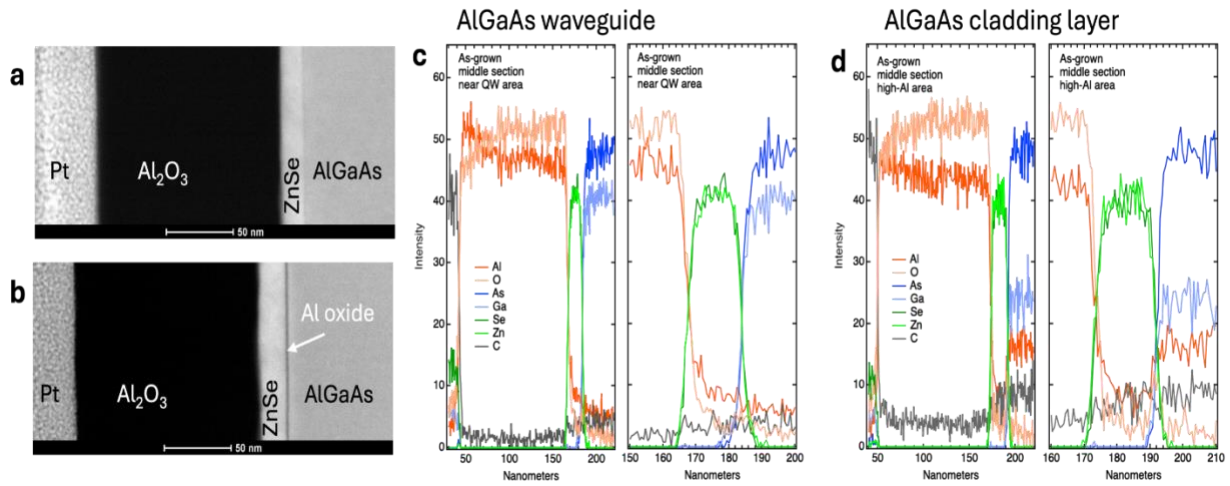

Figure 3. Cross-sectional transmission electron microscopy (TEM) images of an as-grown laser bar obtained in the a. AlGaAs waveguide with low Al concentration, and b. AlGaAs cladding layer with high Al concentration. Elemental profiles across the layer stack measured by energy dispersive spectroscopy (EDS) are show in c. for the corresponding image in a and d. for the corresponding image in b.

Electron channeling contrast imaging (ECCI) in a scanning electron microscope was further used to reveal changes in defects in the ZnSe layer as a function of growth conditions. Figure 4 shows representative images from two laser bar facets that contain ZnSe layers grown at different temperatures. In one set, facets form in the ZnSe grown over the GaAs substrate region. In the other set, the facets are largely absent, but there is now evidence of SeO_x islands at the surface. All samples show evidence of dislocation and/or stacking fault defects in the ZnSe layers. These measurements provided information about how the ZnSe layer growth evolves and the structural features these layers may contain. While the ZnSe layers are highly defective in the region directly over the epitaxial laser bar layers, the impact of those defects in the very thin ZnSe layers that are typically used in the devices was not determined as part of this work, as it is difficult to systematically change their concentrations.

Overall, the structural and chemical characterization applied as part of this project indicates incomplete cleaning of AlGaAs (110) surfaces by the cleaning procedures used by Trumpf. There is an inherent tradeoff when selecting cleaning conditions. Conditions that are not aggressive enough may leave excess oxide at the ZnSe/AlGaAs interface, while those that are strong enough to completely remove the oxide may also damage the QW at the facet. Despite the existence of residual oxide on parts of the facet and extended defects in the ZnSe layer, Trumpf has indicated that these aspects may not be the most immediate source of laser bar failure.

This report is available at no cost from NREL at www.nrel.gov/publications.

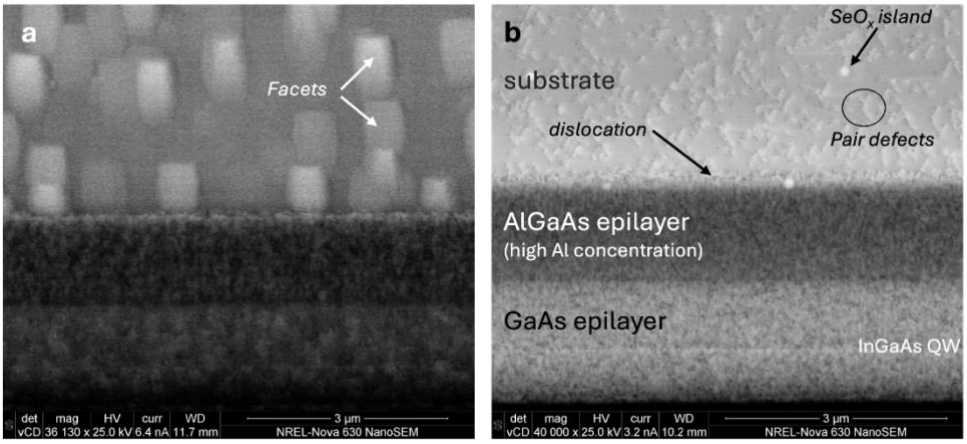

Figure 4. Electron channeling contrast images (ECCI) of two laser bar facets with thick ZnSe layers grown at a. high, and b. low temperatures.

In the second half of this project, work shifted to analyzing aged laser bars to identify the origins of performance loss and failure during operation. The incorporation of a ZnSe passivation layer in the facet design creates the possibility of new sources of defects that lead to failure. Trumpf has observed that laser bars prepared with one set of ZnSe process conditions fail after a significantly reduced time compared to a second set of conditions. One hypothesis is that sub-optimal process conditions may introduce defects that permit greater elemental diffusion across the interfaces of the layers making up the laser facet, leading to unwanted laser light absorption and excess heating. Experiments were designed to examine changes in the elemental profiles across the facet lasers as a function of initial process conditions and operation time measured by Trumpf.

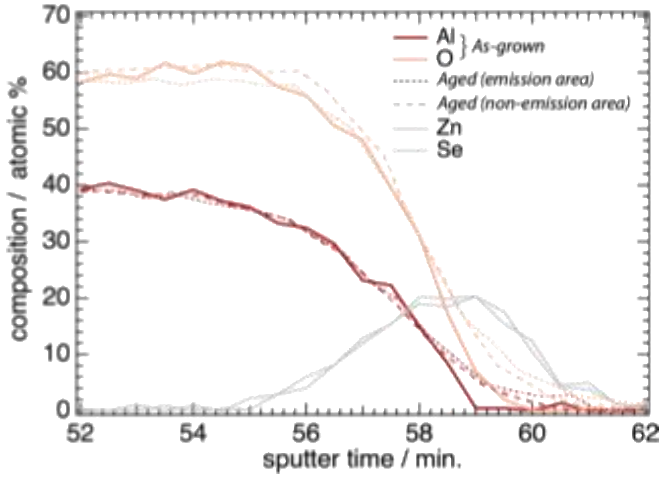

Figure 5. AES elemental profiles across the Al2O3/ZnSe interface in as-grown and aged laser bars. Two regions of the aged laser bars were measured: within the portion of the facet over the light-emitting quantum well, and with the portion of the facet over the GaAs substrate.

The need to drive the degradation process requires measurements to be carried out on the laser facets rather than larger, planar samples processed under similar conditions. These facets are roughly 300 microns x ~1 mm in total area, with a much smaller portion associated with the light-emitting QW region. This required us to adapt existing techniques and sample mounting

This report is available at no cost from NREL at www.nrel.gov/publications.

procedures to properly measure them on such small areas at the end of the laser bar. AES spectra measured across representative as-grown and aged laser bars are shown in Fig. 5. This measurement is capable of high spatial resolution but only measures elemental concentrations at the atomic percent level or higher. Al, O, Zn and Se profiles indicates that Al and O from the Al_2O_3 layers may diffuse slightly into the underlying ZnSe layer during operation (in both the light-emitting and substrate regions). To further assess interdiffusion on lower concentration levels, TOF-SIMS measurements were carried out. This technique is also capable of spatial mapping, although the counts were integrated over a larger spatial window to obtain a reasonable signal. Figure 6 presents elemental profiles measured from three samples: as-grown laser bars, aged laser bars processed under conditions that lead to long lifetimes and aged laser bars processed under conditions that lead to short lifetimes. The profiles suggest some Se may diffusion from the ZnSe layer into the underlying GaAs substrate and device epilayers. Al and O from the Al_2O_3 layer also appear to diffuse at even higher concentrations (although at subatomic percent levels) into the III-V substrate and device layers specifically in the aged laser bar with short lifetimes. Together, the AES and TOF-SIMS measurements suggest that the aged laser bars with short lifetimes undergo higher degrees of elemental diffusion across the interfaces. However, these measurements do not yet point to a root cause, and it is recommended that many more laser bars be sampled under similar measurement conditions to confirm the differences.

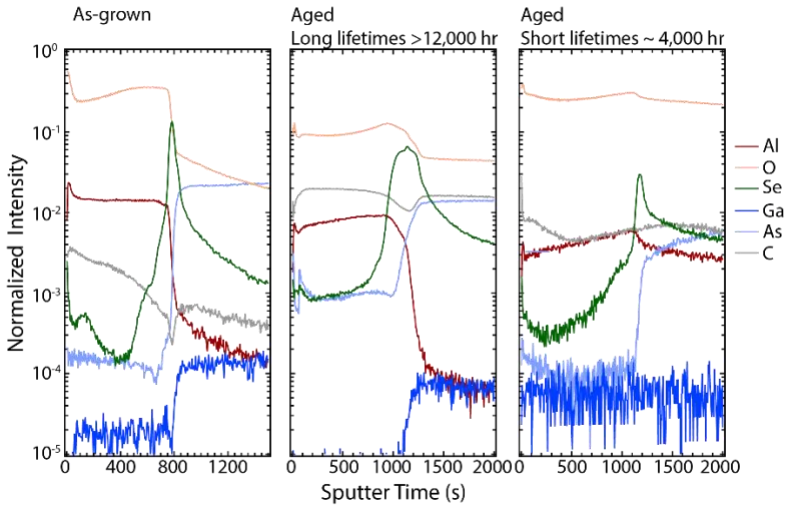

Figure 6. TOF-SIMS profiles across the Al_2O_3/ZnSe/(Al)GaAs interface of (left) and as-grown laser bar, (center) an aged laser bar processed under conditions that lead to long lifetimes, and (right) an aged laser bar processed under conditions that lead to short lifetimes.

A smaller subset of laser bars were also examined with TEM. Figure 7 shows cross-sectional images through the QW region of two laser bar samples: aged laser bars processed under conditions that lead to long lifetimes and aged laser bars processed under conditions that lead to short lifetimes. A main noticeable difference between the two is that the QW within the aged laser bar with a short lifetime looks to be less well-defined than the QW within the aged laser bar with long lifetime. Analysis of additional aged laser bars should also be conducted to determine if this trend is consistent for these process conditions.

This report is available at no cost from NREL at www.nrel.gov/publications.

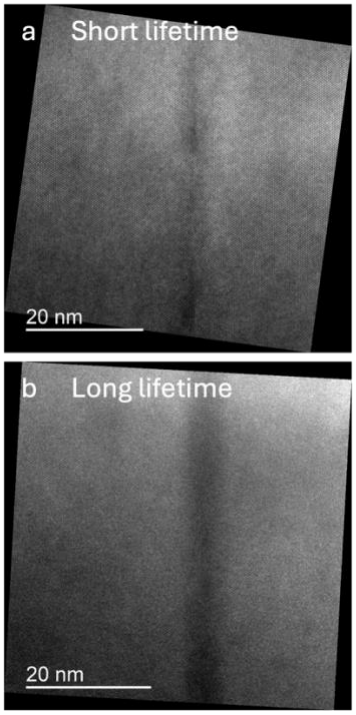

Figure 7. Cross-sectional TEM images of the QW near the facet of two laser bars processed under conditions that lead to: (a) short lifetimes, and (b) long lifetimes.

In total, completed work addressed the main questions and objectives outlined for Task 1. It confirmed that oxygen contamination remains in at least some of the regions of the ZnSe/AlGaAs interface and provided more detailed information about interface intermixing and structural defects in the ZnSe layer. Work at NREL also provided information about oxygen contamination at the Al_2O_3/ZnSe interface and identified ways to mitigate it. Finally, changes to the interface structure and chemistry occurring during laser operation were examined and correlated with the as-grown starting conditions. These studies provide valuable information about the most important aspects of laser bar processing that must be improved via future research and development activities to continue to improve laser bar lifetimes.

Task 2: Improvement of AlGaAs facet cleaning

Trumpf currently cleans their AlGaAs/InGaAs facets with an atomic hydrogen source prior to ZnSe growth, but it is not clear whether their procedure or source is optimized for removing the native oxide from AlGaAs surfaces. NREL will develop a cleaning procedure that is compatible with Trumpf's overall process flow and equipment. This will involve the following activities:

a. NREL will grow AlGaAs epilayers on GaAs (110) wafers with similar compositions as those used by Trumpf in their laser structures. These AlGaAs epilayers will be used to determine the best cleaning procedure. Optimized AlGaAs growth procedures will be developed in the first 6 months of the project. These procedures will then be used to grow material for WPIIb-c for the remainder of the project.
b. A cleaning procedure for oxide removal from AlGaAs surfaces using NREL's atomic hydrogen source will be developed. *In-situ* reflection high energy electron diffraction (RHEED) and Auger electron spectroscopy (AES) measurements will be used to

This report is available at no cost from NREL at www.nrel.gov/publications.

determine the extent of oxide removal immediately after cleaning as well as the properties of the resulting surface. *Ex-situ* XRD, PL, TRPL, CL, and SIMS measurements will also be used to assess the impact of the oxide removal step on the resulting material quality. TEM analysis may also be performed at Trumpf to confirm oxide removal. The optical and structural properties of the ZnSe and AlGaAs materials produced by the optimized cleaning procedure will be compared to ZnSe/AlGaAs standards grown entirely under ultra-high vacuum (UHV) without exposure to air in order to further assess the impact of the oxide removal step on the interface.

c. Pending the success of the hydrogen cleaning procedure, NREL may also explore alternative cleaning methods, including a combination of wet chemical etching and in-situ exposure to elemental or gas fluxes (i.e Ga flux, chlorine-based gases, etc). Characterization by the same methods outlined in WPIIb will be used to assess the success of these cleaning methods.

Results and Discussion

The molecular beam epitaxy (MBE) system at NREL is equipped with an atomic hydrogen source (aka a HABS cell) that can in principle be used to remove the oxide from III-V semiconductor surfaces prior to epitaxy. An open question is whether it is effective at removing oxide from AlGaAs surfaces, which are known to be resistant to oxide removal. Furthermore, the rate of reactions that contribute to removal are dependent on the crystallographic orientation of the oxidized surface. To test the effectiveness of the HABS cell in removing an oxide from a laser bar facet and develop an effective process recipe, NREL first developed growth of AlGaAs films on GaAs (110) oriented substrates to approximate the laser bar facet. Figure 8 shows AFM and PL measurements of a representative AlGaAs (110) film, confirming suitable and representative surfaces to test the cleaning procedure.

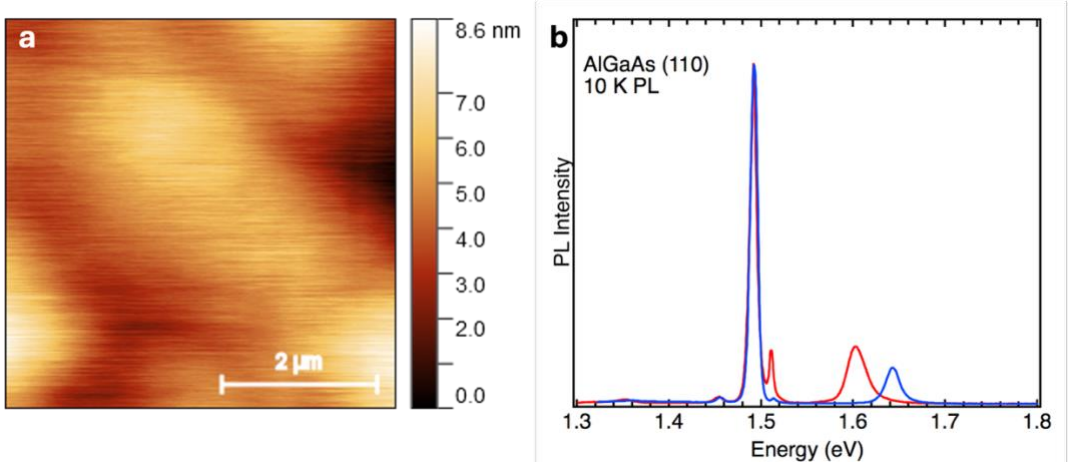

Figure 8. Characteristics of AlGaAs (110) epilayers grown on GaAs (110) substrates a. AFM scan of the surface. b. Photoluminescence of two AlGaAs layers with different Al concentrations.

To approximate the conditions under which Trumpf would utilize the HABS cell for surface cleaning as well as access *in-situ* diagnostics to probe oxide removal during the cleaning procedure, the HABS cell was installed on the MBE growth chamber (as opposed to mounting within a sample preparation chamber, as it is typically implemented). RHEED, AES and low-energy electron diffraction (LEED) were used to assess oxide removal of GaAs and AlGaAs

This report is available at no cost from NREL at www.nrel.gov/publications.

surfaces after various air exposure times, H_2 cleaning conditions and post-cleaning treatments. For example, Fig. 9 shows the RHEED and AES spectra of a subset of GaAs (110) and AlGaAs (110) surfaces with varying oxide thicknesses. Both measurements appear to indicate removal with hydrogen cleaning treatment through the re-appearance of streaks (associated with crystalline surfaces rather than to amorphous oxide surfaces) and the disappearance of an oxygen-related signal, respectively. However, LEED measurements indicate that RHEED and AES may not be sensitive enough to detect complete oxide removal, as shown in the LEED images in Fig. 9e-f. Spots associated with diffraction from clean crystalline surfaces do not strongly appear until ~11 hours into the cleaning procedure.

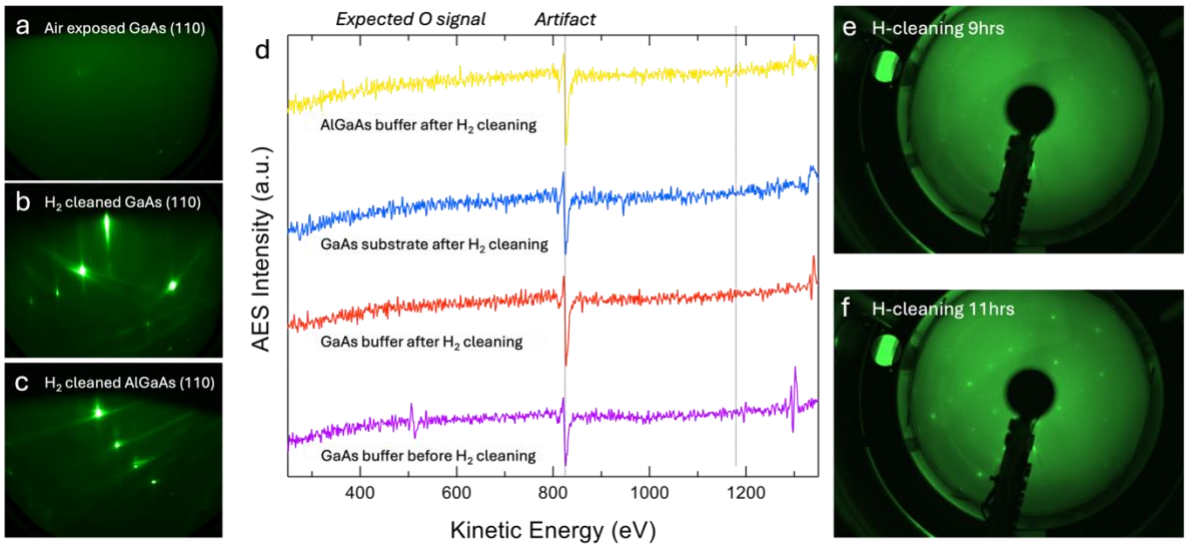

Figure 9. a-c. RHEED images, d. AES spectra and e-f. LEED images of GaAs and AlGaAs (110) surfaces at various stages of hydrogen cleaning.

A hypothesis at the start of this project was that complete oxide removal from the AlGaAs surface was needed to template growth of ZnSe with sufficiently slow defect concentrations to prevent degradation during laser operation. To test the impact of the cleaning on the ability of the (Al)GaAs surface to template high-quality ZnSe growth, ZnSe/(Al)GaAs heterostructures in which the (Al)GaAs surfaces were or were not exposed to air were prepared and assessed with XRD, SIMS and PL measurements. XRD measurements indicate that air-exposed and H_2-cleaned GaAs surfaces produce abrupt interfaces with ZnSe, while air-exposed and H_2-cleaned AlGaAs interfaces do not. SIMS measurements show varying degrees of oxygen contamination at the interfaces of all H_2 cleaned interfaces, although the AlGaAs interfaces exhibit the highest oxygen concentration. Figure 10 shows the associated PL from the ZnSe layers in a subset of these heterostructures. These results are consistent with the TEM images generated in Task 1 of laser bars processed at Trumpf, although the cleaning procedures are different. In the ZnSe/GaAs heterostructures, the ZnSe layer exhibits strong band edge emission but some evidence of additional point and extended defects with longer H_2 cleaning times (Fig. 10a). However, PL reveals very little band edge emission and a very high concentration of defects in ZnSe grown on air-exposed and H_2-cleaned AlGaAs surfaces (Fig. 10c). These results indicate that AlGaAs surfaces are exceedingly difficult to clean sufficiently for high quality ZnSe growth. In fact, the best results were obtained from cleaning that lasted 11-14 hrs at 400 C, which is likely too long

This report is available at no cost from NREL at www.nrel.gov/publications.

to be used in a manufacturing setting and without damaging the underlying device layers. The HABS cell placement was fixed at a distance of 238 mm from the sample surface in the NREL setup, and the cleaning time may be reduced by decreasing the working distance between the cell and sample in a different tool. However, it is unclear whether the decreased distance may ever be able to fully clean AlGaAs surfaces without the use of higher than desired temperatures.

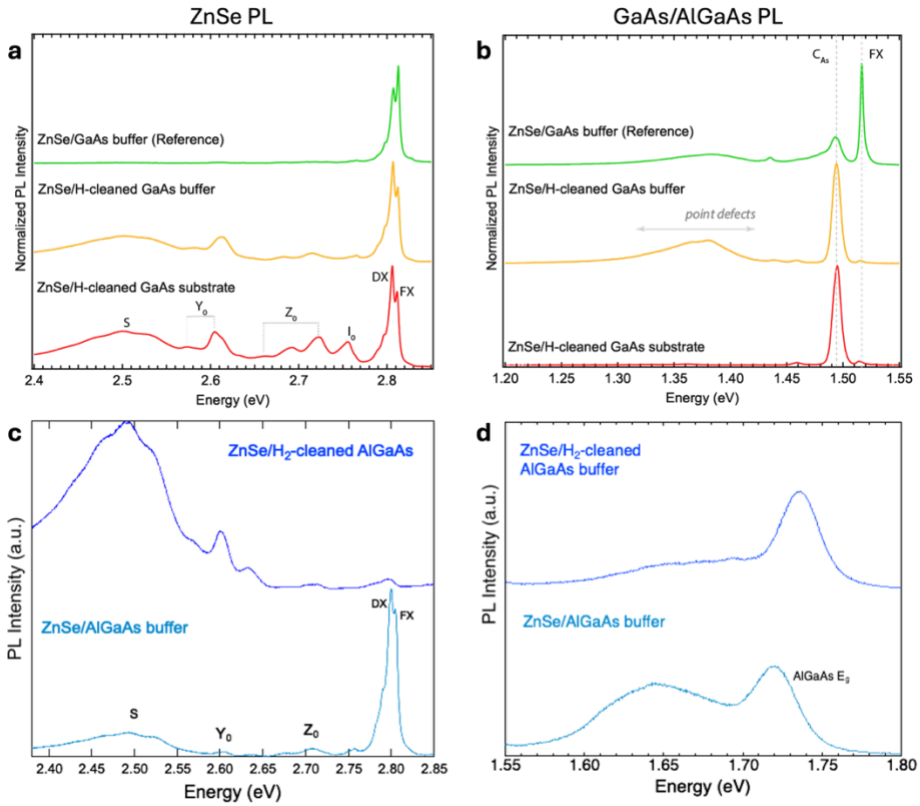

Figure 10. Photoluminescence spectra of ZnSe/GaAs and ZnSe/AlGaAs heterostructures grown with different surface preparation regimes before ZnSe growth. The "ZnSe/GaAs buffer" and "ZnSe/AlGaAs buffer" designations refer to reference samples where the GaAs and AlGaAs surfaces were not exposed to air before ZnSe growth. The GaAs and AlGaAs surfaces of the other samples were exposed to air and the hydrogen cleaned before ZnSe growth. PL spectra are associated with the a. ZnSe and b. GaAs layers of ZnSe/GaAs heterostructures and c. ZnSe and d. AlGaAs layers of ZnSe/AlGaAs heterostructures. The peaks are as follows: FX (free exciton), DX (donor-bound exciton), CAs (recombination from the C acceptor state in GaAs), I0 (deep acceptor-associated recombination), Z0 and Y0 (recombination at extended defects), S (recombination involving impurities).

The overall outcome from work in Task 2 is the recognition that hydrogen cleaning may not be feasibly used to remove all oxygen from AlGaAs surfaces in manufacturing-compatible ways. However, Task 1 suggested that oxygen at the ZnSe/AlGaAs interface may not be the immediate source of laser bar degradation and failure. While other cleaning procedures, such as the use of gases to react with and remove surface oxides, were initially discussed as part of this project, the time, infrastructure and interest did not exist to explore these options further here.

This report is available at no cost from NREL at www.nrel.gov/publications.

Task 3: Epitaxial ZnSe growth

The exact conditions under which ZnSe growth is initiated plays a critical role in its passivation effect on the AlGaAs/InGaAs (110) facet. NREL will determine the correct series of growth initiation steps through the following activities:

a. NREL will first grow ZnSe epilayers (up to 100 nm thick) on MBE-grown AlGaAs (110) surfaces that are protected in UHV from oxidation. The effects of Zn and/or Se pre-treatment steps, II-VI ratios, growth rates and substrate temperature on the resulting material quality will be determined via in-situ characterization (RHEED) and ex-situ structural (XRD, XPS) and optical (PL, TRPL, CL) techniques. The abruptness and bonding environment of the ZnSe/AlGaAs interface, extended defect densities in the ZnSe epilayer, signatures of point defects in the optical spectra of both the AlGaAs and ZnSe epilayers and carrier lifetimes in the AlGaAs layer will be used as metrics in this assessment. TEM analysis on this material at Trumpf will also be used to assess thickness uniformity.
b. NREL will determine the cause of changes in ZnSe epilayer thickness over large areas or arsenide alloy compositions (i.e AlGaAs to GaAs to InGaAs).
c. NREL will identify and quantify in-situ measurement metrics that can be used to assess the material quality of the AlGaAs and ZnSe epilayers and the interface between them.
d. Once the most appropriate growth parameters are found in WPIIIa, these procedures will be applied to air-exposed/cleaned AlGaAs epilayers developed as part of WPII. The same characterization methods will be used to assess the resulting material properties.

Results and Discussion

The conditions under which ZnSe growth is initiated on (Al)GaAs (110) surfaces matter for two reasons. 1) The heterovalent nature of the II-VI/III-V interface can lead to the formation of additional material phases at the interface (for example Ga_2Se_3). 2) Facets are known to form during growth on (110) oriented surfaces due to the specific arrangement of bonding sites on the surface.[1,2] Based on our preliminary understanding developed from previous ZnSe/GaAs (001) growth research at NREL and information in the literature, a simple model was developed to help predict how substrate temperature and Se/Zn ratio will affect the growth mode and incidence of faceting. A simple schematic is depicted in Fig. 11. Conditions that lead to high atom mobility and low nucleation rates, such as low Se/Zn flux ratios and/or higher substrate temperatures, will favor islanding. Conditions that lead to lower adatom mobility and higher nucleation rates, such as high Se/Zn ratios and/or lower substrate temperatures will favor smoother 2D growth modes. This model was used to devise an experiment to further assess how elemental pre-treatment affects the surface morphology, starting first with GaAs (110) surfaces. A pre-treatment of Zn flux prior to the start of ZnSe growth to create a metal-rich environment that supports high adatom mobility was compared to the case where growth was initiated with simultaneous exposure of the GaAs surface to Zn and Se flux (i.e. no treatment). Three different ranges of Se/Zn flux ratios were also used. AFM images of representative growths are shown in Fig. 12. Lower incidence of facet formation was observed for "no-treatment" surface preparation. The metal-rich surface created under a Zn pre-treatment likely increases adatom mobility and leads to increased facet formation for a given Se/Zn ratio. Under a Zn pre-treatment, the RMS surface roughness also decreases as the Se/Zn ratio increases. This outcome is expected, as a high Se/Zn ratio should enhance the nucleation rate and therefore suppresses 3D growth.

This report is available at no cost from NREL at www.nrel.gov/publications.

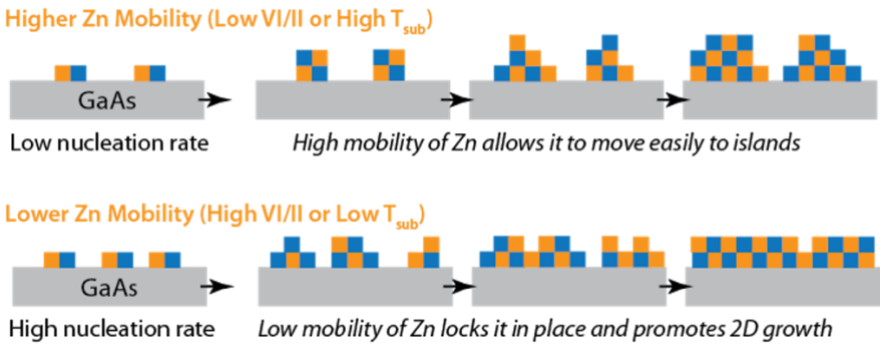

Figure 11. Schematic of growth mechanisms under growth conditions that involve (top) low Se/Zn flux ratios and/or high substrate temperatures and (bottom) high Se/Zn flux ratios and/or low substrate temperatures. These conditions lead to 3D islanding and 2D layer-by-layer growth modes, respectively.

Other aspects of the ZnSe layers and ZnSe/GaAs interface were interrogated by XRD and PL measurements, also shown in Fig. 13. This analysis also contains a Se pre-treatment, where the GaAs surface was first exposed to a Se flux prior to growth. XRD indicates that starting with a Zn-treated surface results in a sharp interface (determined from the presence of pendullosung fringes), while starting with a Se-treated surface causes the ZnSe film to partially relax (determined from the shift in the peak position). Photoluminescence indicates that Zn pre-treatments suppress dislocation formation in the ZnSe layer (notably, the Y_0 emission line associated with dislocations is missing in the ZnSe PL spectrum) and lowers intermixing in the underlying GaAs-based layers (the broad peak < 1.4 eV associated with Zn and Se impurities in the GaAs is relatively lower compared to the excitonic D_0 peak). Comparatively, the absence of a pre-treatment or even the use of a Se pre-treatment increases interdiffusion of Zn and Se into the underlying GaAs layer, increases the dislocations in the ZnSe layer and increases the point defect density in the ZnSe (associated with the presence of the S emission band in the ZnSe PL spectrum). Strain relaxation is known to occur due to the formation of a Ga_2Se_3 interlayer.[3] Cathodoluminescence and ECCI measurements help to confirm the extended defect picture obtained from PL. Representative images, shown in Fig. 14 show that ZnSe grown on GaAs surfaces using a Zn pre-treatment have threading dislocation densities around 10^6 – 10^7 cm^{-2}. The images of ZnSe layers grown without a pre-treatment or using a Se pre-treatment indicate the dislocation densities are much higher, although ballpark values are difficult to obtain when the density is higher than 10^7 cm^{-2}.

This report is available at no cost from NREL at www.nrel.gov/publications.

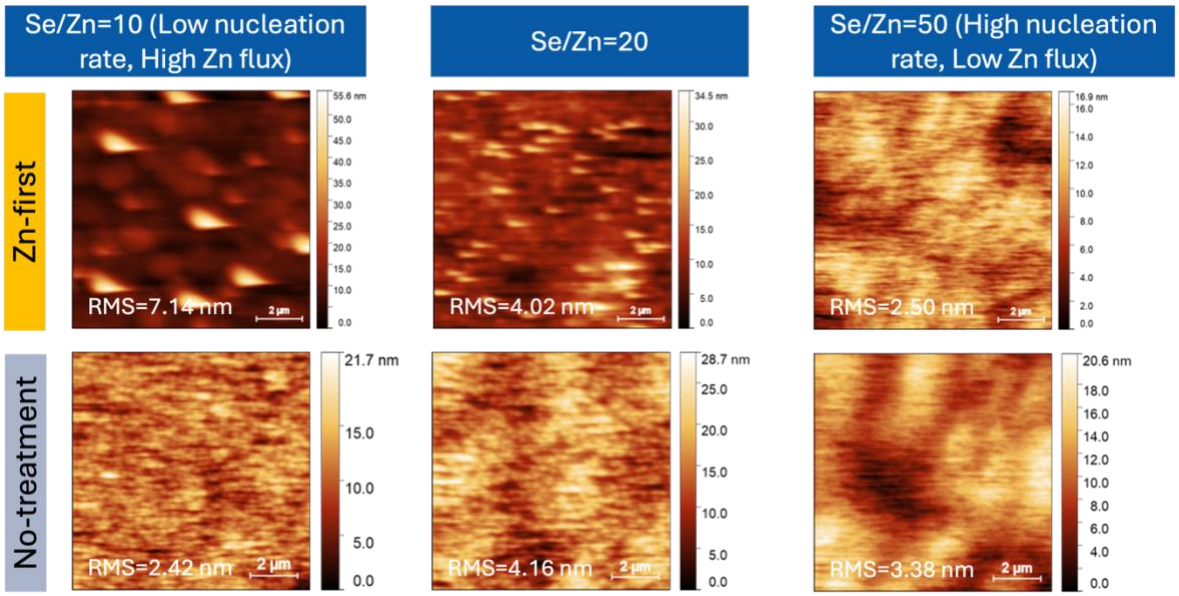

Figure 12. Atomic force microscopy images of the surfaces of ZnSe layers grown on GaAs (110) substrates under different Se/Zn flux ratios. Note: the flux ratio doesn't change the stoichiometry of the ZnSe layer but it does affect the growth mode and resulting morphology.

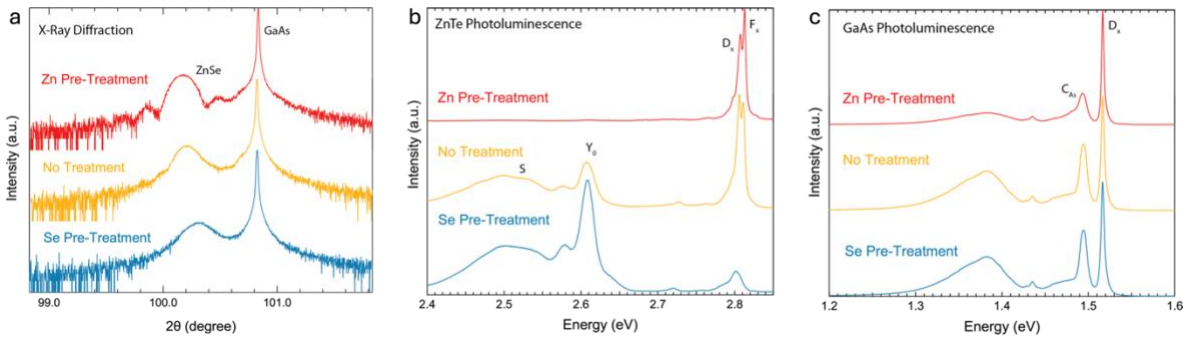

Figure 13. a. X-ray diffraction, b. ZnSe PL and c. GaAs PL from ZnSe/GaAs (110) heterostructures grown with different GaAs surface pretreatment regimes before ZnSe growth.

Subsequent growth on AlGaAs (110) surfaces showed little difference to the growth dynamics or roughness on GaAs (110) surfaces when not exposed to air prior to ZnSe growth (see Fig. 15). Overall, these results suggest there is a trade-off between obtaining an abrupt interface and producing high quality ZnSe (with Zn pre-treatment) and suppressing facets (using no treatment). A brief Zn pre-treatment may provide the best option for achieving an abrupt interface and planar surface.

This report is available at no cost from NREL at www.nrel.gov/publications.

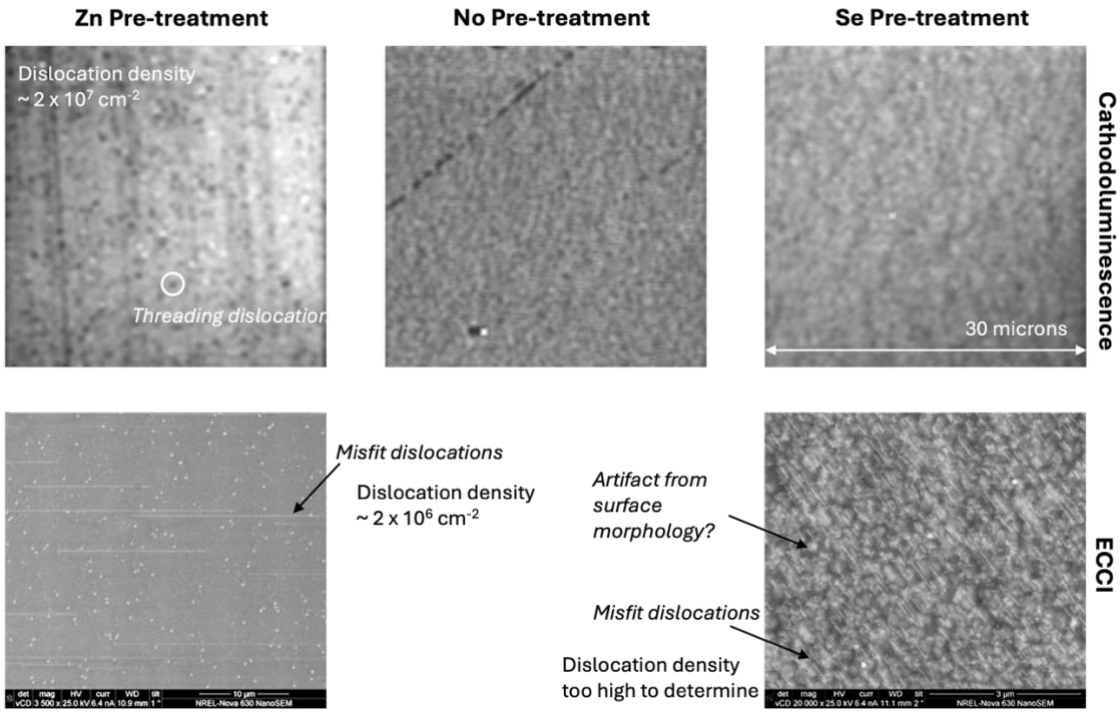

Figure 14. a. (top) CL and (bottom) ECCI micrographs of ZnSe layers grown on GaAs (110) substrates with different GaAs surface pretreatment regimes before ZnSe growth.

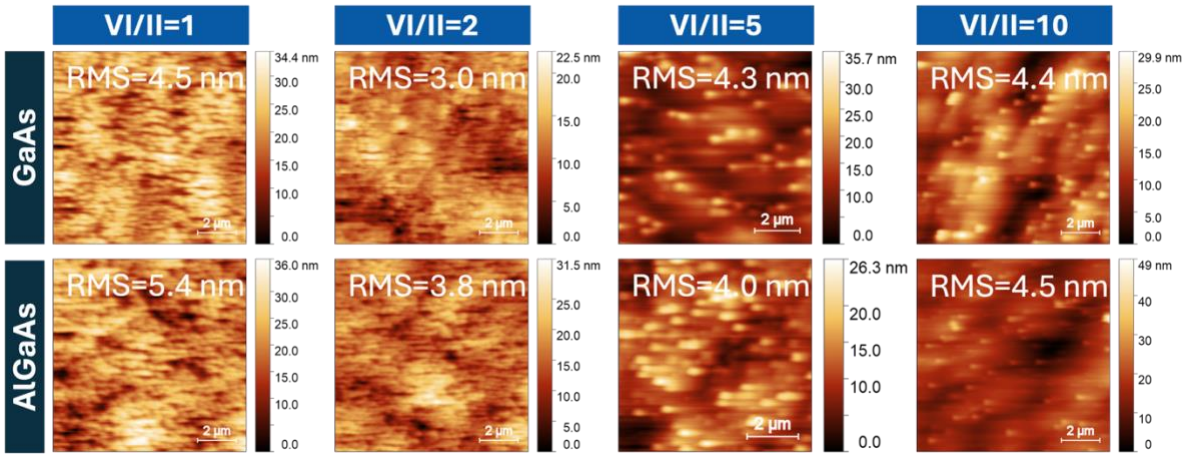

Figure 15. a. Atomic force microscopy images of (top) GaAs (110) and (bottom) AlGaAs (110) surfaces as a function of Se/Zn flux ratios.

This report is available at no cost from NREL at www.nrel.gov/publications.

The ability to determine if the (Al)GaAs surface is optimally prepared for ZnSe growth via *in-situ* measurement techniques is valuable for obtaining repeatable results. From Task 2, we know that oxygen-free (Al)GaAs surfaces support growth of the highest quality ZnSe. Streaky RHEED images are a necessary but not sufficient indicator of an oxygen-free surface and can be used as an initial indicator that the surface is ready for ZnSe growth. Interestingly, during evaluation of the effects of surface pre-treatments, we observed an unexpected behavior, where the GaAs (110) surface exhibited an unexpected reconstruction after Zn or Se pre-treatment. The reconstruction is shown in Fig. 16 and occurs only in instances where the substrate temperature is elevated above 350 C for a brief period of time. Although the origin of the reconstruction is not fully understood at this time, the presence of this reconstruction may be used as a further indicator of a clean surface that will support high quality ZnSe growth.

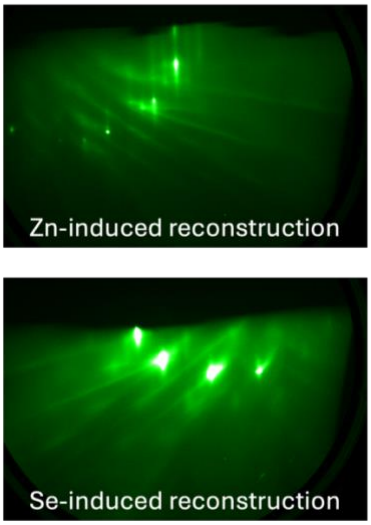

Figure 16. RHEED images of atomic surface reconstructions on GaAs (110) surfaces induced by initial exposure to (top) Zn and (bottom) Se prior to ZnSe growth.

Task 3 initially included a line item to investigate the origin of varying ZnSe film thickness across different layers in the facet. Trumpf later connected the change in thickness to small changes in surface temperature, which are due to differences in thermal conductivity between GaAs, AlGaAs and InGaAs. The ZnSe desorption rate is sensitive to substrate temperature in the approximate temperature ranges used by Trumpf during growth, which fits this hypothesis. NREL did not investigate further.

This report is available at no cost from NREL at www.nrel.gov/publications.

Task 4: Process transfer and reliability verification

Once optimized surface cleaning and ZnSe growth procedures are established in WPII-III, NREL will help to transfer these procedures to the MBE system owned by Trumpf. The effectiveness of these processes will be tested on full AlGaAs/InGaAs laser structures. This is expected to be an iterative process throughout the course of the collaboration. Activities will include:

a. As optimized processes are established at NREL, those processes will be replicated at Trumpf for trial on full AlGaAs/InGaAs laser structures. NREL will help Trumpf to refine the process parameters as needed based on any differences in the MBE systems at NREL and Trumpf.
b. Trumpf will perform lifetime testing on full fabricated laser structures to assess the overall effect of the processing parameters on the laser performance.

Because the cleaning procedures developed at NREL are not appropriate for manufacturing settings and do not represent an improvement over current processing methods used at Trumpf, this task was not pursued as part of this project.

Subject Inventions Listing:

No subject inventions under this CRADA.

ROI#:

None

[1] M.W. Cho, *et al.*, *J. Electron. Mater.*, **27**, 85 (1998)
[2] L.T.P. Allen, *et al., J. Crystal Growth,* **87**, 193 (1988)
[3] D.H. Mosca, *et al.*, *J. Appl. Phys.*, **92**, 3569 (2002).

This report is available at no cost from NREL at www.nrel.gov/publications.